Int J Adv Manuf Technol (2015) 80:477–493
DOI 10.1007/s00170-015-7009-2

ORIGINAL ARTICLE

Experimental investigations into ultrasonic-assisted abrasive flow machining (UAAFM) process

Apurbba Kumar Sharma[1] · **G. Venkatesh**[1] · **S. Rajesha**[2] · **Pradeep Kumar**[1]

Received: 12 November 2013 / Accepted: 10 March 2015 / Published online: 28 March 2015

Abstract Ultrasonic-assisted abrasive flow machining (UAAFM) process is being investigated as an effective variant of traditional abrasive flow machining process. This process aims to achieve better surface finish at higher finishing rate. In this process, a relatively high frequency (5–20 kHz) is provided to the workpiece externally using a piezo actuator. This additional effect is also termed as ultrasonic assistance. Owing to this, the abrasives present in the medium hit the workpiece asperities mostly at an angle and at a higher resultant velocity, thereby making them more effective. In the present work, experiments were conducted on EN8 steels (AISI 1040) to evaluate the process performance of UAAFM on the double acting horizontal type setup. Response surface methodology (RSM) technique was used for designing the experimental plan with four input parameters—applied frequency, extrusion pressure, abrasive mesh size, and processing time. The results obtained after machining by UAAFM were also compared with traditional AFM process. It was found that significant improvements in surface finish could be recorded in UAAFM. The maximum percentage improvement achieved in surface finish was 81.02 %, while maximum improvement in material removal was 0.05 %. The machined surfaces were also investigated using different characterization tools such as scanning electron microscope (SEM), X-ray diffractometer, and three-dimensional optical profilometer.

Keywords Ultrasonic-assisted abrasive flow machining · Response surface methodology · Performance enhancement · Material removal · Surface finish

Symbols

V_a	Axial velocity of abrasive particles (m/s)
F_a	Axial force (N)
V_r	Radial velocity of the workpiece (m/s)
F_r	Radial force (N)
V_R	Resultant velocity (m/s)
F_R	Resultant force (N)
θ	Direction of the resultant force/velocity with respect approximate angle of an abrasive scratch (°)
t	Time (s)
R_a	Arithmetic average surface roughness
F_{res}	Resistance force offered by the workpiece
B	Amplitude
A_s	Shear area
τ_s	Shear strength
μm	Micrometer

Abbreviations

AFM	Abrasive flow machining
USM	Ultrasonic machining
UAAFM	Ultrasonic-assisted abrasive flow machining
MRAFF	Magnetorheological abrasive flow finishing
UFP	Ultrasonic flow polishing
% ΔR_a	Percentage improvement in surface roughness
MR	Material removal

✉ Apurbba Kumar Sharma
akshafme@gmail.com; akshafme@iitr.ac.in

[1] Department of Mechanical and Industrial Engineering, Indian Institute of Technology Roorkee, Roorkee 247667, India

[2] Department of Mechanical Engineering, JSS Academy of Technical Education, Noida, India

SEM	Scanning electron microscopy
XRD	X ray diffraction
RSM	Response surface methodology
FWHM	Full width at half maximum

1 Introduction

Abrasive flow machining (AFM) process plays an important role in many industries involved in precision finishing. The AFM is a well-established nontraditional finishing process in which abrasives are made to flow through a suitably designed fixture. The abrasives that are loosely held in a carrier medium abrades the workpiece surface while travelling in contact with the target surface. A special flexible polymer mixed with abrasives acts as a flexible tool in the process and is termed as medium. Thus, the process allows finishing of small cavities, blind holes, internal surfaces, and intricate shapes of various work materials without having a constraint in workpiece geometry. Owing to such advantages, the process enjoys high demand in wide applications, particularly in precision part finishing and intricate shape machining such as in hydraulic control parts, engine parts, turbine blades, etc. [1, 2].

The basic principles of abrasive flow machining process involve controlled removal of workpiece material by flowing a viscous, abrasive-laden medium under pressure through or across subject surfaces. In most of the conventional AFM machines, the workpiece is held in position between the two opposed medium extrusion cylinders. The abrasive medium is forced back and forth through the passages across the candidate surfaces formed by the workpiece and tooling [3]. This viscoelastic medium carries the force applied by the machine to workpiece edges and surfaces, which form the greatest restriction in the medium's flow path. The machining action produced can be thought of as a filing, grinding, or lapping operation where the extruding slug of abrasive medium becomes a self-deforming stone through the passages restricting its flow. However, the AFM process also has its own limitations such as low finishing rate and low performance while finishing advanced materials. This has resulted in development of few variants of AFM process with superimposed effects.

There are few investigations focused in the direction of improving the efficiency of the processes so as to achieve higher material removal rates by applying different techniques or combining different processes and termed as hybrid abrasive flow machining processes [4, 5]. In some variants, a strong magnetic field had been applied to the workpiece to achieve better finishing rate; in some work, a magnetic rheological fluid was used to improve the surface finish [6–8]. In some other work, a centrifugal force was generated by inserting a centrifugal rod inside the workpiece. In this process, the centrifugal force generating rod is made to rotate about its axis, which in turn rotates the medium and thereby improves the active abrasive grain density [9]. A few researchers inserted helical drill bit flute type to provide helical path to the abrasives; better finishing rates were recorded for these studies [10]. In some other studies, workpiece was rotated and managed to give simultaneous axial and rotary motions to the medium inside the workpiece and finer surfaces at high finishing rate could be achieved compared to simple AFM [11]. One recent innovative approach towards enhancing effectiveness and efficiency was later developed to provide ultrasonic assistance to the workpiece at high frequency during abrasive flow machining process [12].

In the recent years, ultrasonic vibration has become an effective assisting technology in combination with both traditional and nontraditional machining operations. The big disadvantage of the inability to machine nonbrittle materials could be overcome by process assistance of ultrasonic technology [13]. Further, it has also been reported that a number of improved features have been added to the process during various attempts [14, 15]. Mechanics of the process and other aspects of the process including surface finish, roundness, and material removal rate have also been investigated. A few researchers [16, 17] recorded that cutting forces are reduced to 50 % by means of ultrasonic assistance and achieved material removal in smaller and finer chip size, which obviously improves surface finish. In another work, the phenomenon of ductile machining using ultrasonic vibration cutting while working on optical plastics has been reported [18]. Similarly, few researchers reported the significance of vibratory assistance in the application of chip formation, chip braking, drilling, and other processes [19, 20]. The very first ultrasonic assistance with AFM was developed by Jones and Hull [21]. It is a combination of USM and AFM and termed as ultrasonic flow polishing. In this method, the abrasive polymer medium is pumped with a center of the ultrasonically energized tool, and better finishing has been recorded when compared with the simple AFM process.

In the present work, an experimental investigation has been carried out on ultrasonic-assisted abrasive flow machining (UAAFM). It is a new process in which the workpiece is subjected to ultrasonic motion in the perpendicular to the medium flow direction. The high frequency of about 5–20 kHz was given to the workpiece with the help of a piezo actuator and setup. Ultrasonic vibration increases the relative velocity of abrasives, hitting the workpiece surface asperities. This results in more improvement in surface finish and material removal as compared to traditional AFM process. Since the velocity of the workpiece is kept more than the velocity of abrasive particle flow inside, there is a tremendous increase in active abrasive grain density. In addition to this, an additional radial force (F_r) gets added to the process with actuator positioning and mounting in radial direction and perpendicular to the medium flow direction. This arrangement helps the abrasives in getting more depth of penetration into the protruding

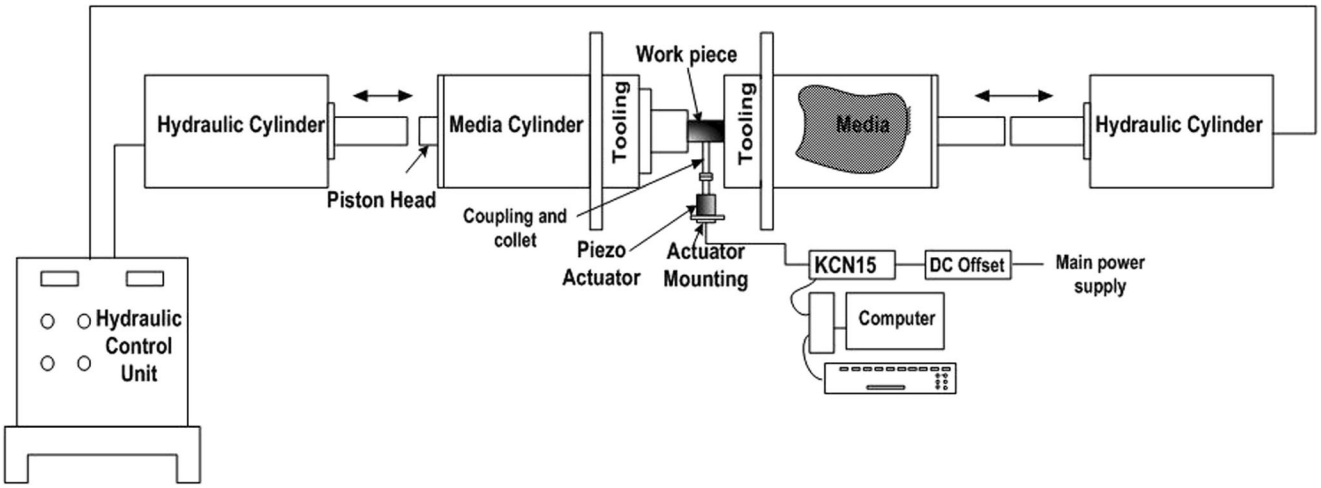

Fig. 1 Schematic view of UAAFM experimental setup

asperities in the plane of vibration; consequently, a marginal improvement in material removal over the classical AFM process could be possible. On the other hand, the parameters such as extrusion pressure and viscosity of the medium will provide sufficient axial forces to the active abrasive grains (F_a) that results in cutting or scratching. The level of abrasive action during the UAAFM process depends on the vibration frequency, extrusion pressure, medium viscosity, number of cycles, and lower amplitude (10 μm). The major advantage lies in the fact that UAAFM provides better surface finish and higher finishing rate (% ΔR_a) as compared to simple AFM for the specified finishing conditions at less time. The surface morphology at different levels of machining was also compared in order to ascertain optimum condition for ultrasonic

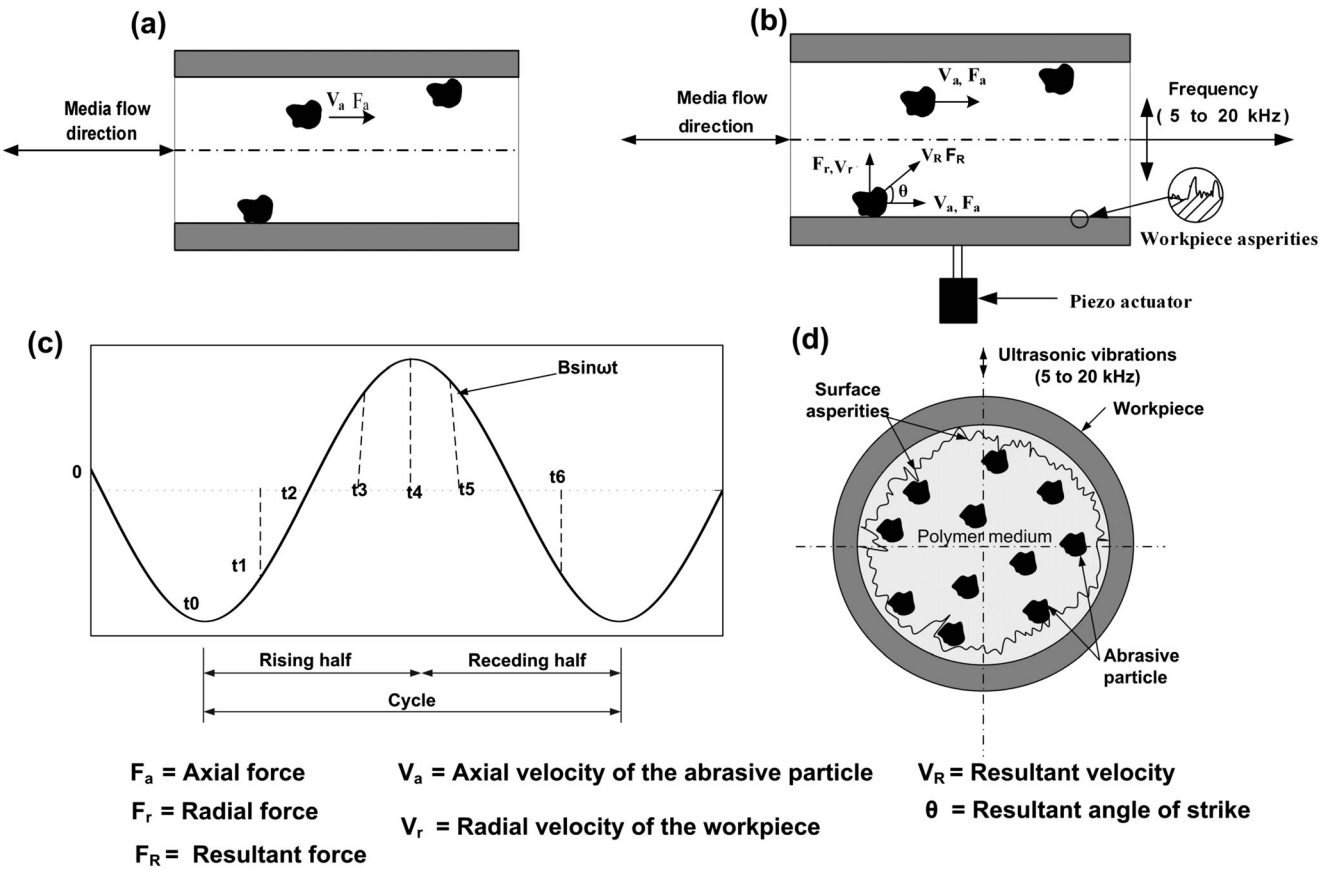

Fig. 2 Forces and velocity vectors in **a** simple AFM, **b** UAAFM, **c** sine wave of rising and receding half of UAAFM, **d** schematic diagram showing the abrasive–asperity interaction in a cross-sectional view of the cylindrical workpiece

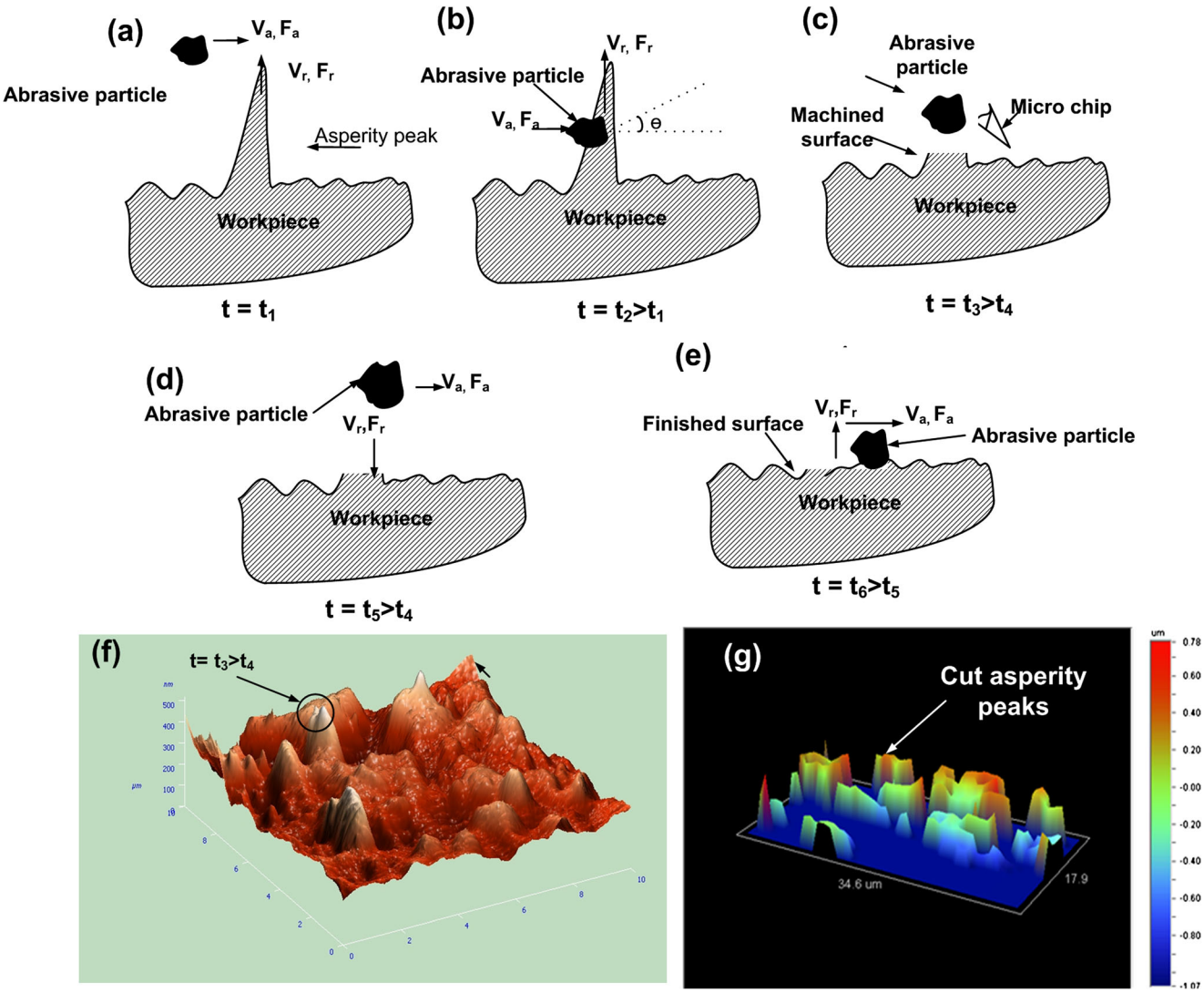

Fig. 3 **a** Different events tends to material removal in UAAFM. **b** Free body diagram of the abrasive–workpiece system. **c** Machined surface. **d** Another event of abrasive–workpiece interaction. **e** Finished surface. **f** Topography of the machined surface obtained through atomic force microscopy. **g** Topography of the machined surfaces obtained through optical profilometer

assistance. In general, 15 kHz frequency (optimum) was found to yield the best surface finish of the machined material. Some aspects of surface integrity of the EN8 steel, finished using UAAFM, have also been investigated.

2 Mechanism of material removal in UAAFM process

The mechanism of material removal in simple AFM process was proposed by many authors, and it is well understood [1–3]. The mechanism include microcutting, owing to abrasion/scratching by the abrasive particles being flown (extruded) under pressure. Further, there are localized plastic deformation due to the pressure applied by the abrasive particles, which get slid or rolled over the workpiece surface but may not actually cause abrasion or microcutting. However, under repeated cycles, some materials get spalled out from the workpiece surface giving rise to microchipping and material removal.

In UAAFM, the workpiece is subjected to vibrations externally using a piezo electric actuator in addition to the conditions of AFM. Hence, the cutting condition never remains the same as in the normal AFM. The piezo actuator is mounted rigidly with the flexible fixture with the support of a center plate of the UAAFM setup. The actuator shaft is connected to the workpiece through coupling and collet as shown in Fig. 1. The actuator is driven by the KC N15-1 amplifier, which is further interfaced with the control computer.

As the abrasive-based medium is pushed from one cylinder to other cylinder in a horizontal type setup, the abrasive contacts through the workpiece axially shown in Fig. 2a; a controlled vibration is introduced to the workpiece in the perpendicular

direction of the medium flow as illustrated in Fig. 2b. In this process, let us consider that the abrasive particles are passing through the cutting direction at a certain velocity V_a (corresponding to the flow rate of the medium maintained during the trials) and force F_a with which they strike the workpiece asperities. Meanwhile, the workpiece also vibrates at a high frequency, orthogonal to the abrasive flow direction. Thus, the velocity of workpiece V_r is also counted during machining. Further, the oscillation (physical movement) of the workpiece in the plane of applied vibration is considerably very high compared to the physical movement of the abrasives axially (in the present work, these values were minimum 5 kHz and 0.053 m/s, respectively). Hence, an abrasive hits a particular asperity peak many times with a resultant velocity V_R while moving perpendicular to medium flow direction as shown in Fig. 2b. In the absence of this additional vibration (Fig. 2a), a small percent of the abrasives will interact with the workpiece surface under the normal applied pressure. Therefore, cutting or material removal shall be governed by the normal AFM conditions. On the other hand, when the workpiece is subjected to external vibrations through the piezo device as illustrated in Figs. 1 and 2b, the interaction between the abrasives and surface asperities will no longer remain similar. The surface asperities thus will be subjected to abrasive action intermittently. Therefore, more number of abrasive cutting edges will be in action at different heights throughout the length of the workpiece; hence, finishing can be achieved at less machining time. The probability of abrasive–workpiece interaction will increase due to advancement of the asperities during the rising half of the applied oscillations (for example, during the events t_1, t_2, t_3, and t_4). Further, the probability shall diminish during the receding half (for example, during the events t_5 and t_6) as shown in Fig. 2c. However, a reverse phenomenon of abrasive–asperity interaction shall take place on the diametrically opposite side of the cylindrical surface in that plane. Thus, there will be possibility of enhanced interaction between the abrasives and the surface asperities during the entire cycle of the applied vibration although not necessarily at the same location. Further, the asperities are randomly distributed over the entire candidate surface as shown schematically in the cross-section of the workpiece in Fig. 2d. Consequently, the abrasive–asperity interaction will take place on the entire internal cylindrical surface throughout the length of workpiece as depicted in the figure. However, as the magnitude of interaction will differ in the planes other than the plane of applied vibration, therefore, the corresponding effect of interaction might vary in the other planes. The current experimental investigation reveals a marginal effect as presented later. The schematic diagram of interactions of the abrasive particles while travelling through the workpiece in UAAFM process is shown in Fig. 3. Possible different events during the interaction of an abrasive particle in the interaction zone shall be primarily determined by the relative velocity of the system as illustrated in Fig. 3a–e. As an abrasive particle moves in its path (Fig. 3a), it may or may not encounter one or more surface asperities. If an abrasive hits an asperity as shown in Fig. 3b, the effective velocity with which it will interact with the asperity shall be at angle "θ." Consequently, a microchip will be produced as illustrated in Fig. 3c. The abrasives precede further (Fig. 3d) with or without interaction with the asperities depending on the real-time surface quality. Eventually, a surface with reduced asperity height (that is, a smother surface, in general) will result as presented in Fig. 3e. The action of the abrasives in an inclined angle is also evidenced by the removal of microchip on workpiece of UAAFM machined surface as observed by means of atomic force microscopy and optical profilometer as shown in Fig. 3f and g, respectively.

In UAAFM, material removal takes place in the form of microchips due to frequent hitting of the asperities by the abrasives at an angle "θ," the angle of inclination of the resultant and chipping as illustrated in Fig. 3b. This results in significant improvement of surface finish as well as material removal. However, as the chip size decreases, the quantity of material removal might not be as significant as that of the surface finish. The resultant angle of strike "θ" on the workpiece will have significant impact on material removal.

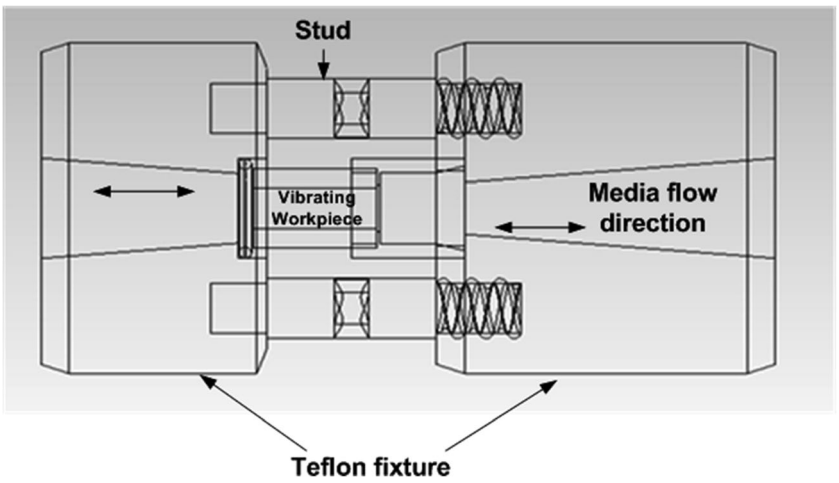

Fig. 4 Special flexible fixture for UAAFM

Let us consider an abrasive with mass "m" hits the workpiece with the force F_R given by

$$F_R = m\dot{V}_R \tag{1}$$

where $\dot{V}_R = \frac{dV_R}{dt}$

The magnitude and the direction of the resultant force (F_R) are then given by

$$F_R = \sqrt{(F_a)^2 + (F_r)^2} \tag{2}$$

and

$$\theta = \tan^{-1}\frac{F_a}{F_r} \tag{3}$$

This force F_R must overcome the shear resistance (F_{res}) of the workpiece in order to cause shearing of the asperity peaks to take place. The resistance offered by the workpiece for removal of material in the form of microchip is given by

$$F_{res} = \tau_s A_s \tag{4}$$

where τ_s is the shear strength of the workpiece material, and A_s is the shear area.

Now, there are three possible cases depending on the magnitude of F_R that influences material removal. These three cases may be as follows:

Case I: If $F_R > F_{res}$, then material is removed in the form of microchip.
Case II: If $F_R = F_{res}$, microplowing may take place.
Case III: If $F_R < F_{res}$, there is no plastic deformation and hence no material removal.

Thus, for a given medium with fixed abrasive size, the relative velocity of the abrasives (V_R) and hence the resultant force (F_R) will largely influence the material removal in this process. The relative velocity is again a function of the applied frequency. It is, therefore, seen that the applied external frequency will have significant effect on the process of material removal.

3 Experimental details

The entire investigation involved extensive experimental work. The experimental procedures adopted are briefly explained in the following sections.

3.1 Machining setup

A two-way horizontal ultrasonic-assisted abrasive flow machine with hydraulic control was used for conducting the trials. The experimental setup was earlier [22] designed and fabricated in the laboratory. A schematic view of UAAFM setup is as shown in Fig. 1.

The UAAFM setup mainly consists of two medium cylinders, two hydraulic cylinders, a specially designed multipurpose tooling for holding a workpiece (Fig. 4), and a piezo (range, 0–20 kHz; model, A125020) actuator with its power supply (KC DC-400) and control unit (KC N15-1). The ultrasonic vibration to the workpiece is provided by the piezo actuator. The actuator is controlled by a computer through the KC N15-1 (Kinetic Ceramics Ltd.), which is powered by KC DC-400 offset. The feed to KC N15-1 was given by a signal generator (make, Tektronix; model no., AFG3252-C) interface. The frequency limit of the device is 0–20 kHz.

The design of workpiece tooling and piezo actuator mounting plays a key role in UAAFM process. The arrangement of workpiece and actuator mounting was tricky in the process. The positioning of the ultrasonic actuator

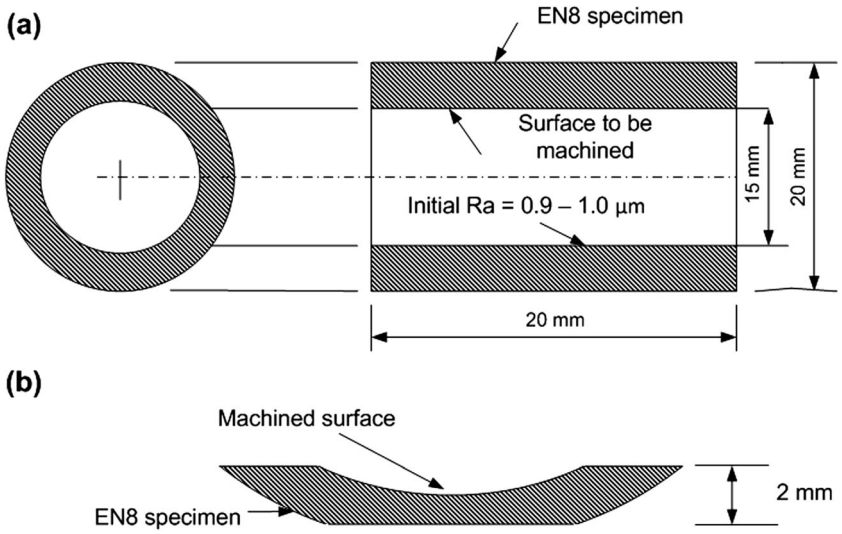

Fig. 5 Sectional views of the workpiece

(axially/radially) will have dissimilar effect on responses in the process. In this work, the actuator was positioned radial to the workpiece and perpendicular to the medium flow direction.

The UAAFM setup was designed keeping in view the flexibility of the process and basic functional requirements. In UAAFM, the medium passes from one cylinder to the other cylinder through the workpiece fixture similar to the simple AFM process. A high frequency of vibration is introduced to the workpiece. The workpiece is kept in dynamic condition while the UAAFM process cycle starts. The medium flow through the cylinders is controlled by the hydraulic control unit.

3.2 Workpiece and media preparations

Selection of workpiece material is basically driven by practical requirement. The EN8 grade of steels is one of the most widely used engineering material, especially used in precision machine tool components where good quality surface is required. Accordingly, EN8 was selected as the workpiece material. The chemical composition of the workpiece was confirmed using an EDS facility. The major elements present in the workpiece are 90.30 Fe, 0.34 C, 7.91 C, 0.63 Si and 0.80 Mn. The EN8 is suitable for the manufacture of parts such as general-purpose collect chucks, nozzles, pin bush coupling, gear molds, and couplings. These components need a considerable amount of processing time for finishing. Hollow cylindrical workpieces of dimension 20 mm (OD)× 15 mm (ID)×20 mm (length) were used for the trials. The samples were prepared by drilling, followed by boring operation. Two sectional views of the workpieces used for the UAAFM trials are shown in Fig. 5a. Figure 5b illustrates a typical sectional view of the machined workpiece prepared for surface characterization through the X-ray diffractometer (XRD) and scanning electron microscope (SEM). Adequate care was taken so that the machined surface does not get damaged; the sample sizes (thickness, 2 mm) were maintained as per the requirements of the measuring devices. The locations of samples for scanning were randomly selected.

In the AFM process, medium plays a key role; it acts as a self-deforming tool. In the present work, a newly developed environment friendly alkene-based medium was used. The major elements of medium are natural organic polymer mixed with SiC particles and naphthenic-based processing oil [23]. The 60:40 ratio (abrasive/carrier) was maintained to achieve the desired medium concentration by weight (wt-%). The weight percentages of abrasive particles and natural polymer were maintained constant throughout the experiment at 60 and 35 %, respectively. The processing oil weight percent was varied marginally (4–5 %) to maintain the desired medium viscosity. In the present work, medium viscosity of 710 Pa s was used and maintained constant throughout the trials. Other constant parameters were maintained at an amplitude of applied vibration of 10 μm, medium flow rate of 560 cm^3/min, and processing temperature at 32±3 °C.

Table 1 Process parameters and their levels used in the trials

Coded values	Applied frequency (*A*) (kHz)	Extrusion pressure (*B*) (bar)	Abrasive mesh size (*C*) (mesh)	Processing time (*D*) (min)
−2	0	2	150	4
−1	5	7	200	5
0	10	12	250	6
1	15	17	300	7
2	20	22	350	8

Table 2 Experimental data

A	*B*	*C*	*D*	% ΔR_a	MR (mg)
15	17	300	5	65.36	11.52
5	7	200	7	52.34	12.21
10	12	250	6	52.13	12.56
10	12	250	4	52.28	9.286
10	22	250	6	51.32	13.09
15	17	200	5	63.45	12.12
10	12	250	8	68.15	12.34
20	12	250	6	66.31	13.04
15	17	300	7	74.92	11.82
5	17	200	5	60.21	12.78
5	17	300	5	50.13	12.31
5	17	300	7	44.12	11.19
15	7	200	7	77.34	14.51
10	12	150	6	71.12	13.04
10	12	250	6	51.01	12.28
15	7	300	5	53.93	10.31
10	12	250	6	55.21	12.31
10	12	250	6	53.04	12.02
10	12	250	6	57.23	12.13
0	12	250	6	26.12	10.58
5	7	200	5	50.21	9.21
5	7	300	7	46.18	9.12
10	2	250	6	45.11	10.23
5	7	300	5	34.56	8.62
15	7	200	5	55.43	10.23
15	17	200	7	63.45	13.67
10	12	250	6	59.12	12.03
10	12	250	6	56.12	12.01
5	17	200	7	51.21	13.45
10	12	350	6	66.46	9.81
15	7	300	7	80.12	12.04

Table 3 The ANOVA for the fitted RSM model for % ΔR_a

Source	Sum of squares	Degree of freedom	Mean square	*F* value	Prob>*F*	
Model	4013.03	14	286.59	48.72	<0.0001	Significant
Residual	94.14	16	5.88	–	–	–
Lack of fit	43.30	10	4.31	0.51	0.8369	Not significant
Pure error	51.06	6	8.51	–	–	–
Cor. total	4107.17	30	–	–	–	–

Standard deviation=2.54, R^2 =0.9781; mean=56.57, adjusted R^2 =0.9570; coefficient of variation (%)=4.48, predicted R^2 =0.9227; predicted residual error of sum of squares=346.11, adequate precision=30.725

3.3 Measurement and characterization

The weight of a specimen was measured using a digital weighing machine (make, Shimadzu; model, AUW220D; accuracy, 0.01 mg). The internal surface roughness of the cylindrical workpiece was measured approximately at the same locations before and after finishing (AFM or UAAFM). Five measurements, approximately spaced at 72° differences along the circumference, for each sample were carried out, and average R_a was considered. The initial average surface roughness of the workpiece was measured using a precision perthometer (make, Taylor/Habson; gauge range, 300 μm; and resolution, 0.01 μm). The range of initial roughness was 0.9–1.0 μm. The percentage improvement in surface finish (% ΔR_a) and material removal (MR) were calculated using the Eqs. (5), (6), and (7) as follows:

$$\%\ \Delta R_a = \frac{\text{Initial}\, R_a - \text{final}\, R_a}{\text{Initial}\, R_a} \times 100 \tag{5}$$

$$\text{MR} = [\text{Initial weight} - \text{final weight}] \tag{6}$$

$$\%\ \textit{improvement in MR} = \frac{\text{Initial weight} - \text{final weight}}{\text{Initial weight}} \times 100 \tag{7}$$

The Bruker AXS D-8 advanced diffractometer was used to obtain the X-ray diffractometer spectra of the machined surfaces in order to assess the phases present and to determine the changes, if any, on the UAAFM machined surfaces due to machining. A scanning electron microscope (SEM; model, FEL Quanta 200) was used for examining the surface topography of the machined surfaces. The samples were sectioned longitudinally along a small chord with a thickness of 2 mm (thus, length of the sample remains the same at 20 mm) so that the machined surface becomes visible to the sensory system of the measuring device, and the sample can be placed on a flat mounting surface. The schematic of a typical prepared sample is illustrated in Fig. 5b and Section 5.5.

4 Selection of process parameters and experimental design

As discussed earlier, central composite rotatable design (CCRD) was used to plan the experiments on UAAFM. Four major input parameters, i.e., applied frequency (*A*), extrusion pressure (*B*), abrasive mesh size (*C*), and processing time (*D*) (Table 1), were selected. Analysis of the experimental results was performed using standard response surface methodology (RSM). Parameters and their levels were selected based on their significance obtained through preliminary studies and set up constraints. Applied frequency and processing time were two introduced input parameters for the first time in any AFM investigation by Rajesha et al. [22]. In RSM, a relationship between a response and the process parameters is represented by a higher order polynomial Eq. (8).

$$Y = b_0 + \sum\nolimits_{i=1}^{k} b_i x_i + \sum\nolimits_{i=1}^{k} b_{ii} x_i^2 + \sum\nolimits_{i<j-2}^{2} b_{ij} x_i x_j \pm \varepsilon_r \tag{8}$$

where *Y* is the output response (say, % ΔR_a), b_0, b_i, b_{ii}, and b_{ij} are coefficients, ε_r is the experimental error, and x_i are the independent input parameters [24].

Table 4 The ANOVA for the fitted RSM model for MR

Source	Sum of squares	Degree of freedom	Mean square	*F* value	Prob>*F*	
Model	63.48	14	4.53	82.16	<0.0001	Significant
Residual	0.96	16		0.060	–	–
Lack of fit	0.71	10	0.070	1.72	0.2622	Not significant
Pure error	0.073	4	0.018	–	–	–
Cor. total	64.35	30	–	–	–	–

Standard deviation=0.25, R^2 =0.9850; mean=11.67, adjusted R^2 =0.9719; coefficient of variation (%)=2.10, predicted R^2 =0.9308; predicted residual error of sum of squares=4.45, adequate precision=35.769

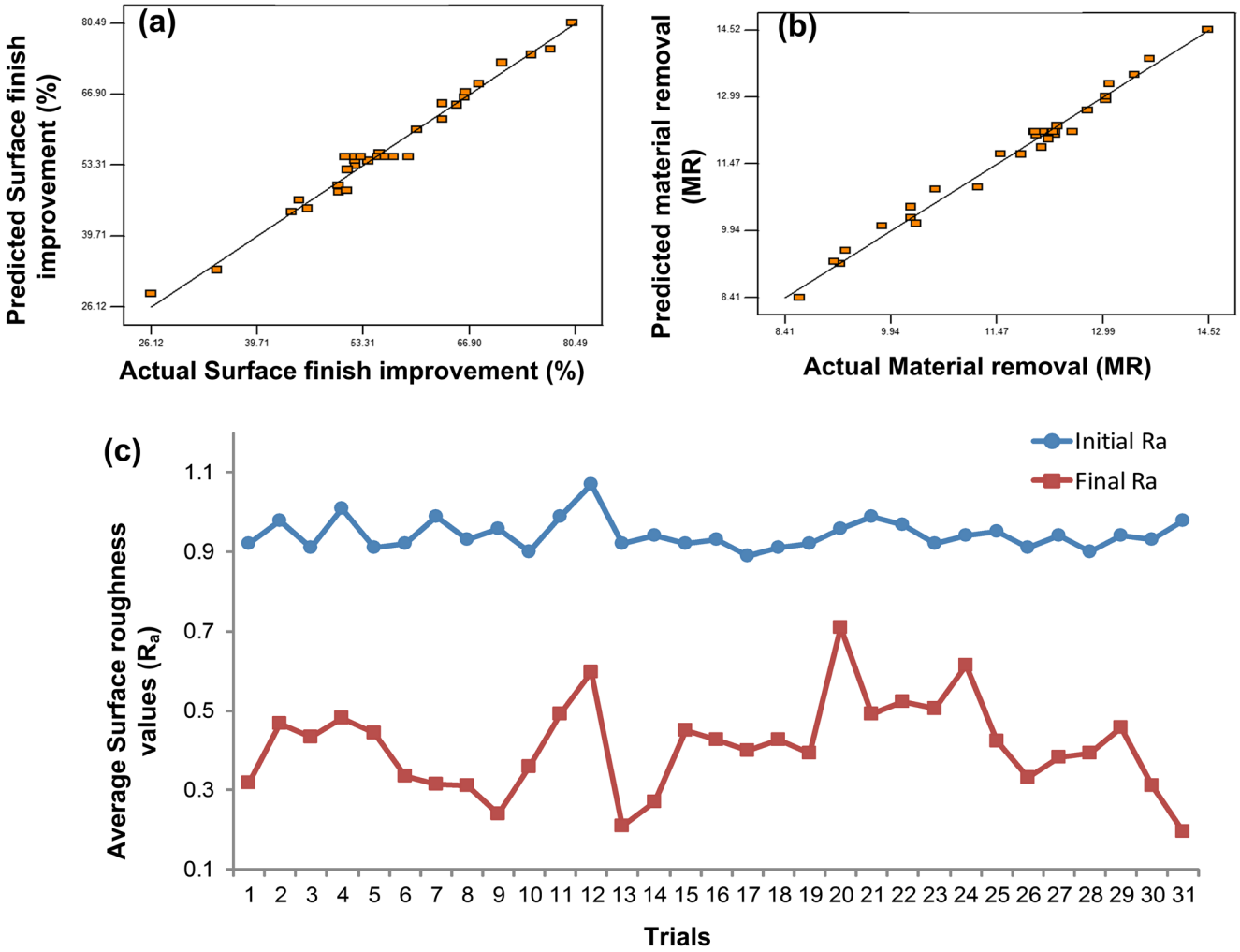

Fig. 6 Plots of best fit for actual values against predicted values for responses. **a** Surface finish improvement. **b** Material removal. **c** Average arithmetic mean (R_a) values corresponding to the initial and final machining conditions

The machining data are tabulated in Table 2. The responses were analyzed using a widely accepted commercially obtainable software tool (Design Expert 6).

4.1 Regression analysis

The relation between the input variables of UAAFM and the responses such as surface finish (% ΔR_a) and MR as derived by the analysis tool based on the experimental data can be expressed in terms of coded values and are represented in Eqs. 9 and 10, respectively.

Surface finish improvement (% ΔR_a),

$$\begin{aligned}\%\Delta R_a = {} & +228.54-3.75*A+6.14764*B-1.17*C \\ & -21.54*D-0.074*A*A-0.05*B*B+1.52\text{E}-003*C*C \\ & +1.64*D*D-0.06*A*B+0.02*A*C+0.74*A*D \\ & +4.18\text{E}-003*B*C-0.84*B*D+0.033*C*D\pm\varepsilon\end{aligned} \quad (9)$$

Material removal (MR),

$$\begin{aligned}\text{MR} = {} & -27.92-0.041*A+1.03*B+0.08*C+7.75*D-3.03057*E \\ & -003*A*A-4.53*E-003*B*B-6.88*E-005*C*C-0.33*D*D \\ & -0.022*A*B+3.92\text{E}-004*A*C+0.06*A*D+2.25*E \\ & -004*B*C-0.10*B*D-0.01*C*D\pm\varepsilon\end{aligned} \quad (10)$$

where "ε" represents an experimental error, and A, B, C, and D are the coded parameters as defined in Table 1.

The regression and fitted quadratic models were determined using the analysis of variance (ANOVA) for both surface finish improvement and material removal, and the results are tabulated in Tables 3 and 4, respectively. The ANOVA results reveal that the quadratic model and the process parameters chosen for the experimentation are statistically significant. Figure 6a and b shows the results of model application by plotting values of the collected data points with respect to the model's predicted positions—additional verification points were sourced by adopting the missing experimental configurations of the central composite from the response

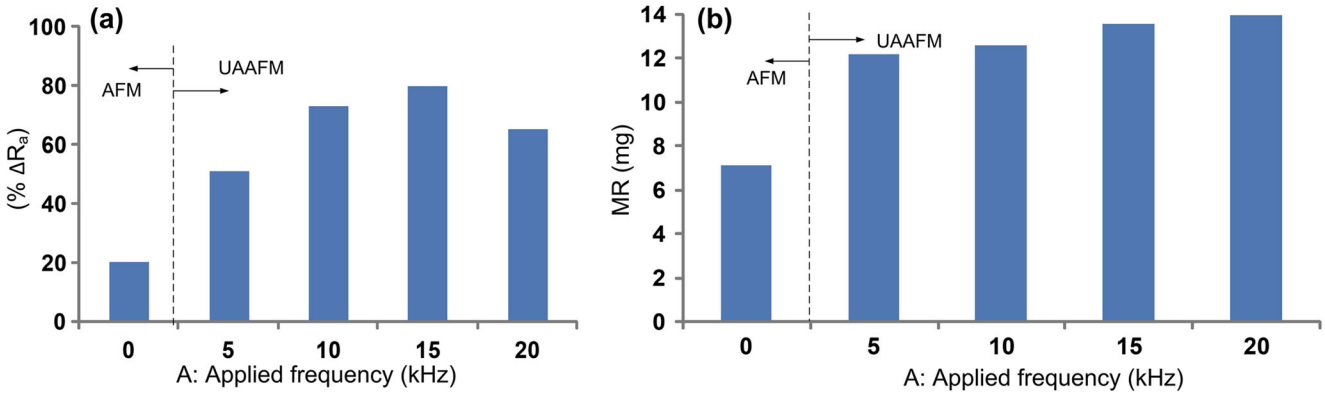

Fig. 7 Comparison of AFM and UAAFM in terms of **a** improvements in % ΔR_a and **b** MR (processing conditions: extrusion pressure, 12 bar; abrasive size, 250 mesh; and processing time, 6 min)

surface methodology technique. The actual data are within the range of ±15 of the predicted values. This is indicative of higher degree of correlation. Further, the experimentally obtained values of the surface roughness corresponding to the initial and final machining conditions are presented in Fig. 6c. It may be noted here that the samples were prepared (bored) with the target of maintaining the range of initial roughness within 0.9–1.0 μm; the machining conditions, thus, were set accordingly. Consequently, a relatively uniform surface with low scatter could be seen. The final surface finish profile, on the other hand, represents the measurements obtained at different machining (trial) conditions according to the CCRD. It is clear from the data (Fig. 6c) that the average roughness of the surface got reduced significantly (R_a=0.41 μm) after the UAAFM; however, the changes in the roughness values were influenced considerably by the variations in the trial conditions (Table 2). The overall scatter of the final roughness values was 0.12.

5 Results and discussion

The results obtained are discussed in the following sections.

5.1 Finishing through AFM and UAAFM processes

The prefinished cylindrical specimens were finish-machined using the simple AFM and UAAFM modes of machining. Experiments were conducted to study the effects of input parameters to on the process performance of AFM and UAAFM in terms of % ΔR_a and MR (mg). The corresponding results are presented in Fig. 7. It may be noted that % ΔR_a and MR are significantly higher in UAAFM process as compared to simple AFM process. The observed low finishing rate in AFM while compared to UAAFM may be attributed to negligible radial force. The abrasive particles move along the axis of cylindrical workpiece leading to relatively less interaction with the workpiece surface. In the UAAFM process, on the

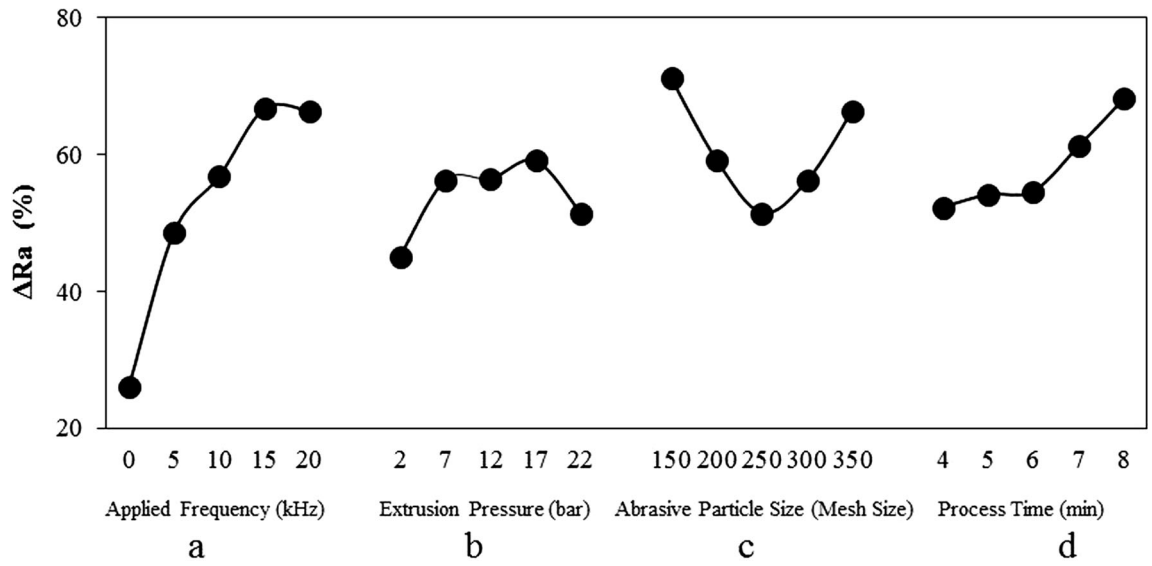

Fig. 8 Response curves showing the effect of process parameters on surface finish improvement

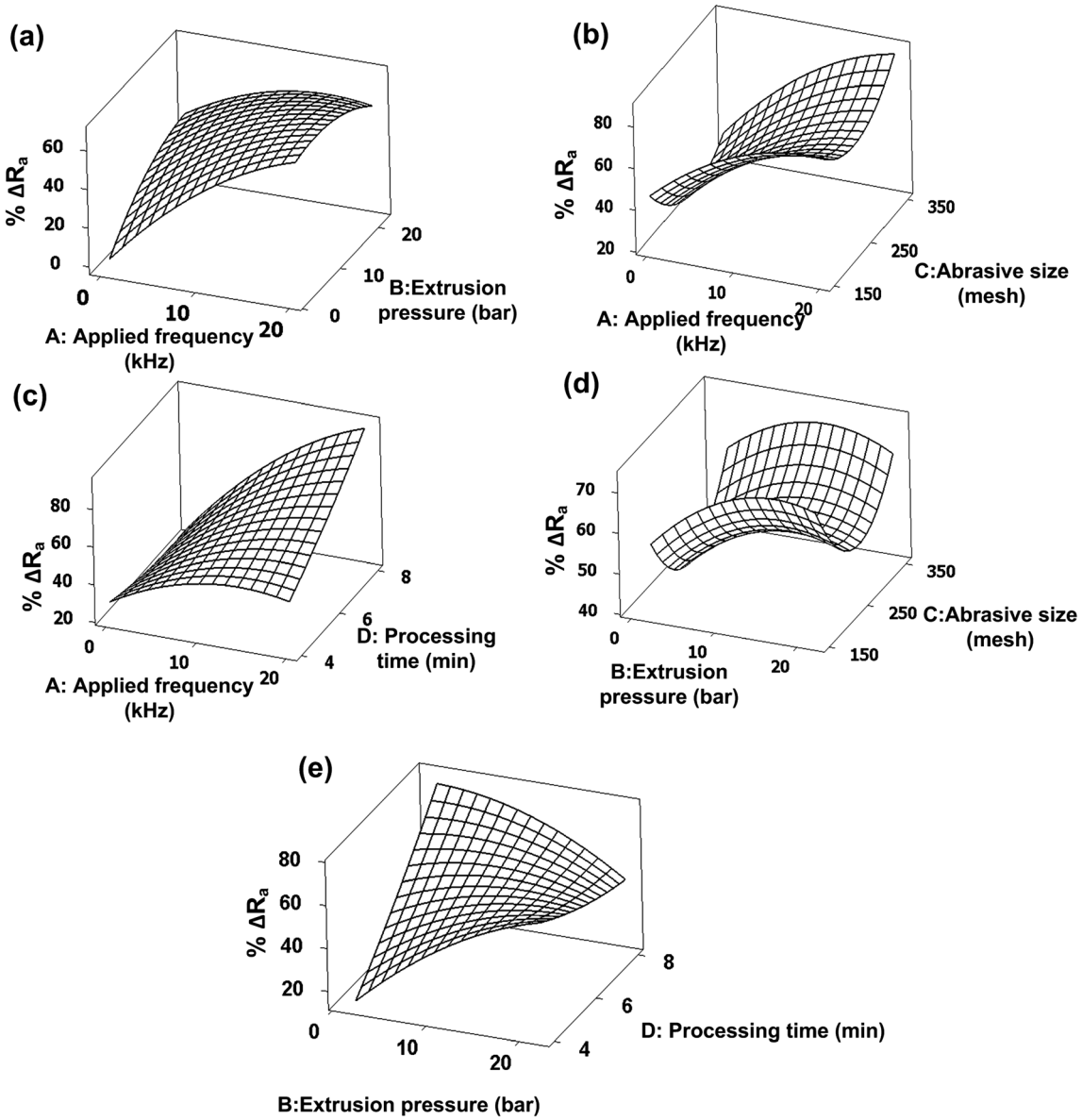

Fig. 9 Surface response plots for surface finish improvement and combined effect of **a** applied frequency and extrusion pressure, **b** applied frequency and abrasive mesh size, **c** applied frequency and processing time, **d** extrusion pressure and abrasive mesh size, and **e** extrusion pressure and processing time

other hand, the workpiece is in dynamic condition, which is made to vibrate radially at high frequency, and consequently, it is subjected to additional radial force along. The radial velocity of the workpiece gets added to the velocity of the abrasives in the axial direction and contributes towards observed changes in surface finish improvement and material removal as discussed in Section 2.

5.2 Effect on surface finish improvement

The externally applied vibration frequency combined with other parameters like extrusion pressure, processing time, and abrasive mesh size, and some constant parameters like medium viscosity, medium flow rate, etc. are the major parameters in this work that had contributed to the machining of EN8 material. Results show that the major contribution to improve surface finish was by the high frequency vibration applied to the workpiece. Statistical analyses show that the applied frequency is one of the significant parameters for the RSM model. The results are shown in the Tables 3 and 4.

Figure 8 shows the main plot effect of the process parameters selected for the trials on improvement of surface finish. It was observed that, as the applied frequency (A) increases, surface finish is also increased up to 15 kHz and attains maximum value (Fig. 8a). Beyond this value, no significant

improvement in % ΔR_a is observed. As the vibration frequency increases, number of asperity peaks coming in contact with the flowing abrasive grains increases; hence, more asperity peaks of finer sizes get removed. Further, it is to be noted that the cycle time is fixed for the given extrusion pressure). In other words, % ΔR_a had been increased. However, beyond the maximum value, the surface attains a glazed texture, and further increase in workpiece frequency might cause deterioration of the finished surface. The trend is similar for the extrusion pressure; surface finish improves with increase in pressure initially and then starts falling down (Fig. 8b). Such results have been discussed at length elsewhere [25]. The observed trend curve with respect to abrasive mesh size parameter shows that % ΔR_a is increasing owing to removal of large asperity peaks by the impact of the relatively coarser abrasives. Further the machined surface quality becomes again better with finer abrasive particles (>250 mesh) as illustrated in Fig. 8c. At this stage, the finer particles are even removing the fine peaks resulting in a glazed surface. On the other side, % ΔR_a increases with increase in processing time as exhibited by the characteristics at Fig. 8d.

The combined effects of the process parameters on the output have been illustrated in the form of response surfaces in Fig. 9. It is observed from the figure that the applied ultrasonic frequency had the highest contribution in surface quality with 26–80 % variation. It is, however, observed that the improvement in surface finish appears saturated with an applied workpiece vibration of 15 kHz beyond which the effect is only marginal. The data also reveal that the extrusion pressure has the minimum influence on the changes in surface quality (45–55 % variation only) for the investigated range. Finer abrasives are always preferred as indicated by the larger improvement in the finer surfaces (R_a values are in ranges of 0.2–0.5 μm). Higher processing time (Fig. 9d, e), on the other hand, yields better machining performance; higher applied frequency and higher extrusion pressure may not be advisable in combination with higher processing time.

5.3 Effect on material removal

Figure 10 illustrates the individual effect of the parameters such as ultrasonic frequency, extrusion pressure, abrasive mesh size, and processing time on material removal using UAAFM process. It is observed from the trend curves that there is an increase in MR with an increase in frequency (Fig. 10a) due to the fact that, at high frequency, the workpiece asperities experience impact of the abrasives particles at an angle that facilitates easy shearing of the peaks. It has been already discussed in Section 2 (Fig. 3) that material removal through shearing becomes easier owing to the additional radial component of the velocity. Similarly, the trend curve for extrusion pressure follows that of the applied frequency. The curve with respect to abrasive mesh size parameter shows the established trend that MR decreases with increase in mesh size as shown in Fig. 10c. On the other hand, MR increases with increase in processing time in general. However, MR gets saturated beyond 6 min of machining owing to the onset of glazing of the machined surface. At this stage, not many large asperities will be present on the workpiece surface, and hence, there is hardly an increase in MR as evidenced in Fig. 10d. Further, it is worth mentioning that the AFM and UAAFM processes are basically finishing processes; hence, only marginal changes in the MR values were obtained.

The surface response plots for material removal are presented in Fig. 11. It is observed from the figure that the material removal increases with an increase in ultrasonic frequency and extrusion pressure (Fig. 11a). It is also observed from the surface plots (Fig. 11b) that the material removal decreases with the increase in mesh size; this is due to the fact that larger

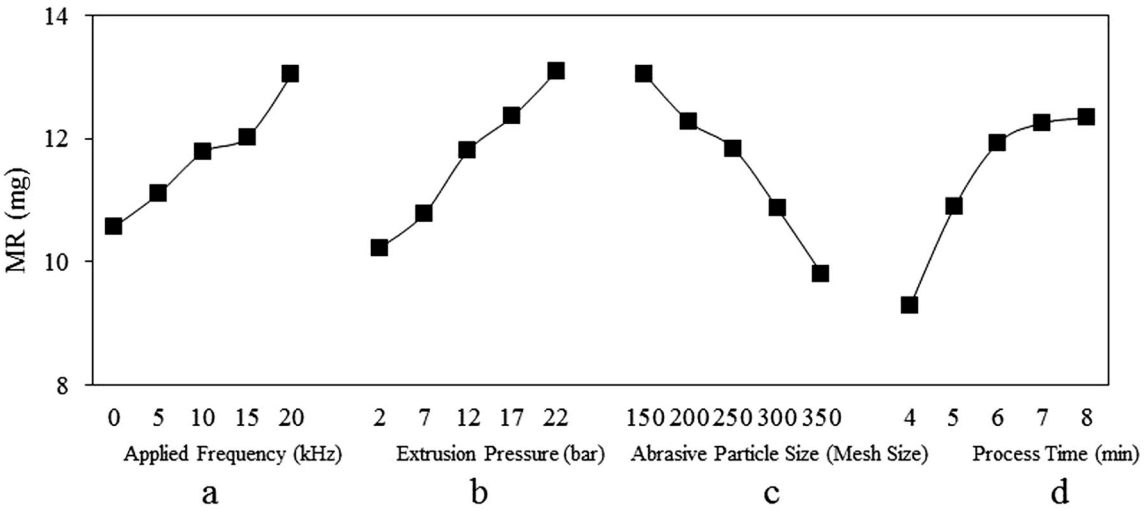

Fig. 10 Response curves showing the effect of process parameters on material removal

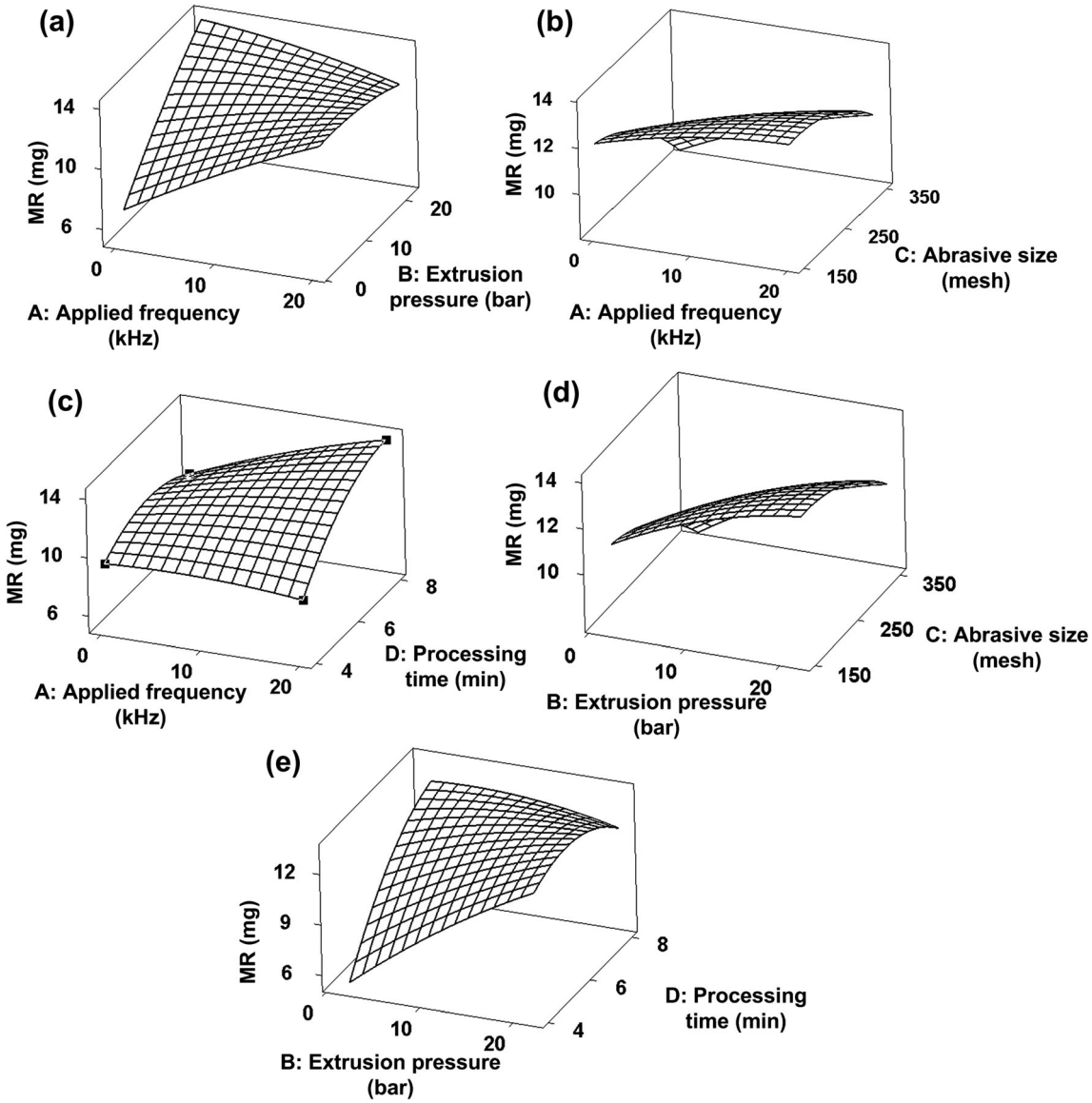

Fig. 11 Surface response plots on improvement of material removal and combined effect of **a** ultrasonic frequency and extrusion pressure, **b** ultrasonic frequency and abrasive mesh size, **c** ultrasonic frequency and processing time, **d** extrusion pressure and abrasive mesh size, and **e** extrusion pressure and processing time

particles possess higher energy $\left(=\frac{1}{2}mv^2\right)$ with which they will interact with the surface asperities on the workpiece. Higher processing time provides more interaction with the active abrasives; accordingly, the surface plots show improvement in the MR with increase in applied frequency (Fig. 11a–c). Material removal does not get improved with processing time even in combination with extrusion pressure as the surface gets glazed slowly (Fig. 11d, e).

Table 5 XRD data of the UAAFM processed specimen

Machining conditions	2-Theta of the first major peak (°)	FWHM of the first major peak (°)
Preabrasive flow machined surface	44.8964	0.1309
Simple AFM (0 kHz)	44.6185	0.1870
5 kHz	44.1755	0.2244
10 kHz	44.7589	0.2244
15 kHz	44.8991	0.2964
20 kHz	44.9609	0.3149

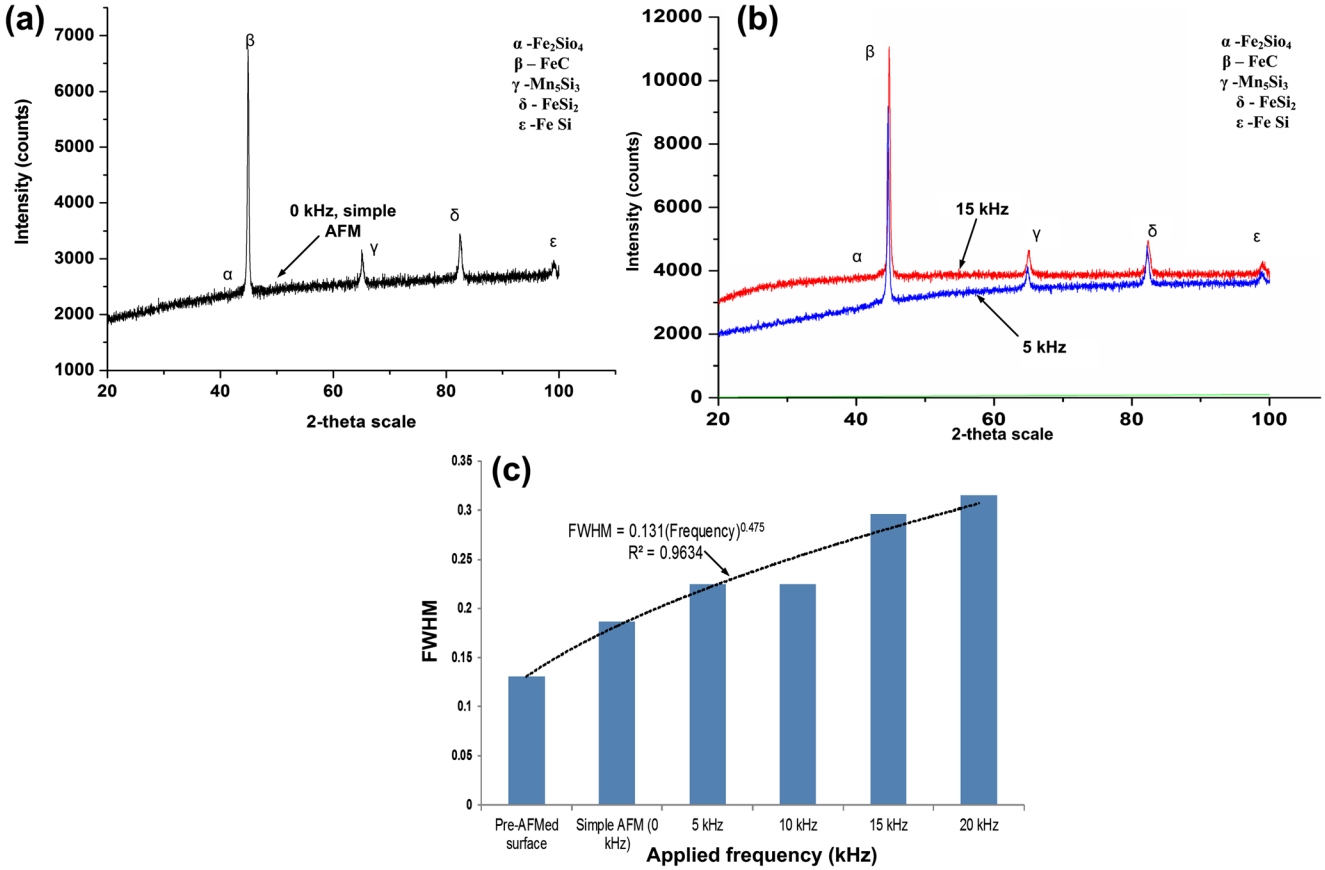

Fig. 12 **a** X-ray diffraction patterns of the EN8 specimen processed through UAAFM at 5 kHz applied frequencies. **b** Observed shift in the peaks on the XRD spectra of workpiece machined (0 kHz) and after machined at 20 kHz. **c** Variation of FWHM with the change in frequency

5.4 X-ray diffraction analysis

The XRD technique has been exploited effectively by many researchers for the evaluation of the machined surfaces [26–28]. An analysis through X-ray diffraction was carried out to identify the changes on the workpiece surface during the finishing operation under different applied ultrasonic frequencies. Diffraction patterns were obtained by a Bruker AXS D-8 advance diffractometer with Cu K_α radiation and nickel filter at 20 mA and 35 kV. The specimens were scanned with a step time of 0.5 s. The corresponding results are presented in Fig. 12. The results of machined surfaces worked at different UAAFM conditions are shown in Table 5. The analysis shows that FeC, Fe_2SiO_4, $FeSi_2$, FeSi, and Mn_5Si_3 are the major phases regularly present in the EN8 steel before and after processing the workpieces. The results show that the most dominating peak of the machined workpiece was observed around 44° on the 2-theta scale. The minor shift of the major peaks with a marginal change in the 2-theta value was observed with increase in the applied frequency during processing (Fig. 12b). This shift in peaks would generally vary with the externally applied loads (i.e., straining and hence stresses get induced in the material). In the present work, an external frequency was applied to the workpiece. It is observed that the induced stresses are different at different applied ultrasonic frequency as indicated by the observed shift in the major peaks. The trend is found similar with the results for centrifugal force-assisted AFM [26].

The full width at half maximum (FWHM) values of the first major peaks of the spectra were computed and presented

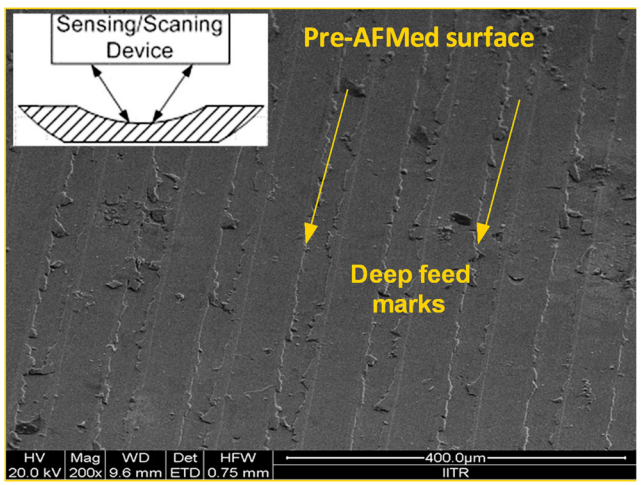

Fig. 13 Micrograph of pre-abrasive flow machined surface. *Inset* Schematic of a typical prepared sample

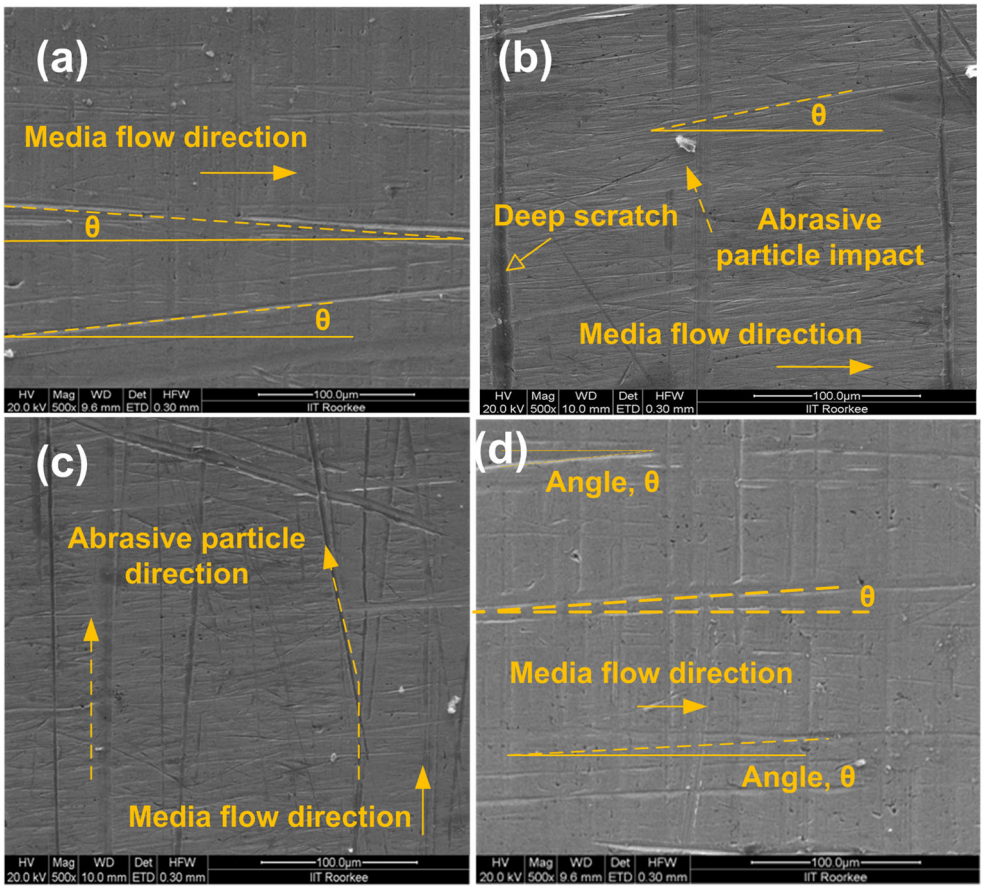

Fig. 14 Typical SEM micrographs of the ultrasonic-assisted abrasive flow machined surfaces at different applied ultrasonic frequencies: **a** 5 kHz, **b** 10 kHz, **c** 15 kHz, and **d** 20 kHz

in Table 5. Correlation of the full width at half maximum of XRD of the monitored profiles with residual stresses has been reported by Vashista and Paul [29]. The FWHM is generally correlated to state of stress, plastic deformation in the work material, and grain size. The results of the present study reveal that the FWHM typically increases with an increase in applied frequency as shown in Table 5 and Fig. 12c, although the trend suggests that the increase in the FWHM is nonlinear (a power correlation was obtained to fit the observed data with good correlation, R^2=0.9642). The increase in the FWHM can be correlated to probable increase in the residual stresses on the machined surfaces [29]. This is attributed to the fact that, at high frequency, the abrasive particles interact with the work surface at higher velocity; this results in higher plastic deformation on the work surface as well as changes in the grain sizes on the machined surface. The higher strain is manifested as the broadening of the XRD peaks as shown in Fig. 12b. The results show that the maximum value of the FWHM corresponding to the peak obtained from the spectrum is at 20 kHz applied frequency. However, as the surface gets glazed early at higher applied frequency (say, 20 kHz), further improvement in the surface quality becomes marginal as discussed already (Figs. 7 and 8). As the major asperities get removed and the surface attains a better topography, the straining of the surficial grains gets reduced even at higher applied frequency leading to the flattening of the curve at Fig. 12c.

5.5 Scanning electron microscopy analysis of machined surface

Scanning electron microscopy was used to observe the topography of the machined surface. Figure 13 shows a typical surface of a EN8 steel workpiece prior to machining through UAAFM. The conventional boring marks are clearly visible on the machined surface. The additional ultrasonic assistance provided externally to the workpiece in AFM process will make the abrasives more active in the work volume. The abrasives hit the surface asperities continuously at an angle "θ" as discussed earlier. This angle of scratch in finishing zone will depend on the actuator mounting position, medium composition, and geometry of the workpiece used apart from the applied vibration parameters. In the present study, the actuator was mounted radial to the workpiece. The resulting abrasive marks indicating thin direction (scratch at an angle "θ") are shown in the topography of the surface in Fig. 14. It is revealed from the figure that abrasive-scratch direction varies with a change in the applied frequency on workpiece surface. This may be due to the fact that, at high frequencies, there is

increase in active abrasive grain density. As the applied ultrasonic frequency increases from 0 to 5 kHz, the abrasive starts hitting at an angle "θ" as can be seen in Fig. 14a. The observation also confirms the mechanism of machining in UAAFM. As the ultrasonic frequency increases from 5 to 10 kHz, the effect of abrasives hitting the target surface has been increased, whereas the angle of abrasive scratch direction was similar to that of earlier one (as shown in Fig. 14b). It was observed that, with an further increase in ultrasonic assistance, the abrasives cause deep scratches on the target surface (Fig. 14c). At higher frequency, of about 15–20 kHz (Fig. 14d), deeper scratches were observed leading to fall in ΔR_a (Fig. 8a). Moreover, at high frequency, the abrasive particles get less interaction time, and therefore, relatively shorter scratch marks could be clearly observed. This also indicates that a higher applied frequency is not favorable for better surface integrity of the ultrasonic-assisted abrasive flow machined surfaces. Moreover, no visible microcracks other than the scratch surfaces could be identified on the ultrasonic-assisted abrasive flow machined surfaces corresponding to any applied ultrasonic frequencies. This is favorable with respect to surface integrity of the machined surface.

6 Conclusions

Finishing of internal cylindrical surfaces of EN8 steels through UAAFM process has been successfully carried out using a natural polymer medium. The results were also compared with simple AFM process. It was observed that the UAAFM process yields better surface finish at higher finishing rate. The results have been derived using various commercial analysis tools and techniques. Most of the results are presented with help of 3D plots in terms of response surfaces. Thus, these results can be used by other researchers and practitioners in industries for developing their scheme for AFM machining. The optimization shall help them to avoid repetitive works. Results show that an ultrasonic frequency introduced in a conventional AFM plays an important role in improving the effectiveness finishing process.

The following major conclusions can be drawn from this work.

- Surface finish increases with increase in applied frequency up to a level (in this case, 15 kHz), whereas at very high frequency (20 kHz), the percentage improvement starts reducing.
- Material removal increases with the increase in applied frequency and extrusion pressure.
- The most significant factor in UAAFM is the applied frequency that helps in attaining an improvement in surface finish up to 80.12 % at 7 kgf/cm^2 extrusion pressure. The maximum value of MR obtained in UAAFM is 14.5 mg corresponding to 7 min of processing time. This rate of material removal is marginally higher compared with the traditional AFM process, although the process is basically a finishing process.
- The applied ultrasonic frequency causes straining in the top layer of the ultrasonic-assisted abrasive flow machined surface leading to changes in the microstructure of the machined surface as indicated by marginal increase in FWHM values.
- The abrasives hit the target surface at angle "θ." The depth of scratches increases with the increase in applied frequency.
- Relatively low applied frequency is favorable for better surface integrity.

Acknowledgments The authors are thankful to the Department of Science and Technology, Government of India, for providing financial assistance to this work through DST Project Grant No. DST-384-MID.

References

1. Rhoades LJ (1991) Abrasive flow machining: a case study. J Mater Process Technol 28:107–116
2. Rhoades LJ (1988) Abrasive flow machining. Manuf Eng 1:75–78
3. Loveless TR, Willams RE, Rajurkar KP (1994) A study of the effects of abrasive flow finishing on various machined surfaces. J Mater Process Technol 47:133–151
4. Cheema MS, Venkatesh G, Dvivedi A, Sharma AK (2012) Developments in abrasive flow machining: a review on experimental investigations using abrasive flow machining variants and media. Proc ImechE B J Eng Manuf 226(12):1951–1962
5. Mali HS, Manna A (2009) Current status and application of abrasive flow finishing processes: a review. Proc ImechE B J Eng Manuf 223(7):809–820
6. Singh S, Shan HS, Kumar P (2002) Wear behavior of materials in magnetically assisted abrasive flow machining. J Mater Process Technol 128(1):155–161
7. Sidpara A, Jain VK (2011) Experimental investigations into forces during magnetorheological fluid based finishing process. Int J Mach Tools Manuf 51(4):358–362
8. Jha S, Jain VK (2004) Design and development of the magnetorheological abrasive flow finishing process. Int J Mach Tools Manuf 44(10):1019–1029
9. Walia RS, Shan HS, Kumar P (2006) Abrasive flow machining with additional centrifugal force applied to the media. Mach Sci Technol 10(3):341–354
10. Sankar MR, Mondal S, Ramkumar J, Jain VK (2009) Experimental investigations and modelling of drill bit guided abrasive flow finishing process. Int J Adv Manuf Technol 42:678–688
11. Sankar MR, Ramkumar J, Jain VK (2009) Experimental investigations into rotating workpiece abrasive flow finishing. Wear 267:43–51
12. Sharma AK, Kumar P, Rajesha S (2011) An improved ultrasonic abrasive flow machining and a device therefor. Patent number 3578/DEL/201, India, Dec 9
13. Liu K et al (2004) Study of ductile mode cutting in grooving of tungsten carbide with and without ultrasonic vibration assistance. Int J Adv Manuf Technol 24(6):389–394
14. Kei-Lin K, Chung-Chen T (2012) Rotary ultrasonic-assisted milling of brittle materials. Trans Nonferrous Metals Soc China 22:793–800

15. Brehl DE, Dow TA (2008) Review of vibration-assisted machining. Precis Eng 32(3):153–172
16. Nath C, Rahman M (2008) Effect of machining parameters in ultrasonic vibration cutting. Int J Mach Tools Manuf 48: 965–974
17. Nath C, Rahman M, Andrew SSK (2007) A study on ultrasonic vibration cutting of low alloy steel. J Mater Process Technol 192: 159–165
18. Kim JD, Choi IH (1997) Micro surface phenomena of ductile cutting in the ultrasonic vibration cutting of optical plastics. J Mater Process Technol 68(1):89–98
19. Komanduri R, Von Turkovich BF (1981) New observations on the mechanism of chip formation when machining titanium alloys. Wear 69:179–188
20. Deyuan Z, Wang L (1998) Investigation of chip in vibration drilling. Int J Mach Tools Manuf 38:165–716
21. Jones AR, Hull JB (1998) Ultrasonic flow polishing. Ultrasonics 36:97–101
22. Rajesha S (2011) Some studies to enhance the capabilities of abrasive flow machining process. Dissertation, IIT Roorkee, India
23. Venkatesh G (2010) Performance study of a new polymer media for AFM. Dissertation, IIT Roorkee, India
24. Montgomery DC (2004) Design and analysis of experiment. Wiley, New York, pp 427–500
25. Reddy KM, Sharma AK, Kumar P (2008) Some aspects of centrifugal force assisted abrasive flow machining of 2014 Al alloy. Proc ImechE B J Eng Manuf 222(7):773–783
26. Walia RS, Shan HS, Kumar P (2008) Morphology and integrity of surfaces finished by centrifugal force assisted abrasive flow machining. Int J Adv Manuf Technol 39:1171–1179
27. Balart MJ, Bouzina A, Edwards L, Fitzpatrick ME (2004) The onset of tensile residual stresses in grinding of hardened steels. Mater Sci Eng A 367(1):132–142
28. Poggie RA, Wert JJ (1991) The influence of surface finish and strain hardening on near-surface residual stress and the friction and wear behavior of A2, D2 and CPM-10 V tool steels. Wear 149(1):209–220
29. Vashista M, Paul S (2012) Correlation between full width at half maximum (FWHM) of XRD peak with residual stress on ground surfaces. Philos Mag 92(33):4194–4204